Polymer Journal, Vol. 13, No. 4, pp 357—369 (1981)

Crystallite Size Analysis of Pressure-Crystallized Polyethylene by Nitric Acid Etching and Gel-Permeation Chromatography. I. Extended-Chain Crystals

Yoji MAEDA and Hisaaki KANETSUNA

Research Institute for Polymers and Textiles, 1-1-4, Yatabe-Higashi, Tsukuba, Ibaraki 305, Japan.

(Received August 20, 1980)

ABSTRACT: Average crystal thickness and its size distribution in the molecular chain direction of polyethylenes crystallized under a high pressure of about 500 MPa were determined statistically by fuming nitric acid degradation followed by gel-permeation chromatography (GPC) measurement for molecular weight distribution of the degraded samples. The observed GPC curves were corrected for instrumental spreading by Chang-Huang's method in order to estimate precisely the crystal size distributions. Several important facts were found. First, the so-called extended-chain crystals which show a main melting peak at *ca.* 415 K on the DSC curve consisted of two constituents having lamellar thicknesses of highly extended-chain crystals and ordinary extended-chain crystals, which corresponded to the thermal behavior observed before by DSC and high-pressure dilatometry. Second, it was found that the average crystal thickness of ordinary extended-chain crystals is between one half and one third the average thickness of highly extended-chain crystals. Third, it seems that folded-chain structure exists in the ordinary extended-chain crystals having an average thickness of several hundred nanometers.

KEY WORDS Polyethylene / High-Pressure Crystallization / Nitric Acid Etching / Gel-Permeation Chromatography / Instrumental Spreading Correction / Average Crystal Thickness / Crystallite Size Distribution / Highly Extended-Chain Crystals / Ordinary Extended-Chain Crystals /

In the past two decades, the morphology of extended-chain crystals (ECC) of polyethylene crystallized under high pressure has been extensively studied. The only technique used was the observation of replica of the fracture surfaces of the samples by electron microscope. However, the method of fracture surface observation encounters a difficulty when dealing precisely with average crystal thickness and its size distribution in the molecular chain direction of the crystals, since it becomes necessary to compute the statistics of crystal thickness exposed by the many fracture surfaces. This method tends to overlook small crystals and thus results in an estimation of average crystal thickness greater than the actual value. Only a few studies[1,2] came near to solving the statistical problem of the average lamellar thickness and its size distribution of the pressure-crystallized polyethylenes, especially of the ECC crystals.

The new procedure for degrading polyethylene with fuming nitric acid followed by measuring molecular weight distribution (MWD) by gel-permeation chromatography (GPC) proved valuable for understanding the molecular structure of a variety of folded-chain crystals (FCC) of polyethylene.[3,4,5,6] The novel use of GPC for the degradation products of polyethylene offers a rapid means of recording the whole MWD in the course of degradation. This procedure was applied to measuring the crystal size distribution of ECC of polyethylene by Illers[7] and Bassett *et al.*[8] However, in these works, the GPC instrumental spreading effect on the observed GPC curves was neglected so that accurate data could not be obtained.

The present study deals with a quantitative analysis of the molecular chain extension of the cyrstalline lamellae of polyethylenes crystallized from the melt under a high pressure of about 500

MPa.

EXPERIMENTAL

Materials

The material used in this study was Sholex S 6002, a linear polyethylene with a weight-average molecular weight M_w of 165,000 and a weight- to number-average molecular weight ratio M_w/M_n of 5.2; it was supplied by Showa Denko Co. Samples were crystallized from the melt at 513 MPa in a high-pressure dilatometer described in detail elsewhere.[9]

Methods of Investigation

In order to follow the oxidative attack by fuming nitric acid, the weight loss, density, and viscosity-average molecular weight of a sample were measured as a function of degradation time. The weight loss was determined by weighing the sample before and after the treatment. The density was measured in a density-gradient column of toluene and chlorobenzene at 298 K. While doing so, the sample underwent a change in molecular weight (MW). The viscosity of the original sample was measured in decalin at 408 K with a Ubbelohde dilution viscometer. The viscosity-average molecular weight M_v was calculated from the intrinsic viscosity $[\eta]$ *vs.* MW relationship established by Chiang[10]:

$$[\eta]^{\text{decalin}}_{408\,\text{K}} = 6.2 \times 10^{-4}\ M_w^{0.70} \qquad (1)$$

Calorimetry was carried out with a Perkin-Elmer DSC II differential scanning calorimeter at a heating rate of $5\,\text{K}\,\text{min}^{-1}$. The temperature was calibrated within ± 0.5 K by using the melting point standard of indium 429.6 K and that of lead 600.4 K. Then melting temperature was taken to be the peak temperature on the DSC curve.

Nitric Acid Degradation

The oxidation method of Palmer and Cobbold[11] was used in this study. The polymer in bulk was oxidized at 353 K in a sealed flask with a large excess of Analar-grade fuming nitric acid (*ca.* 94% concn., $1.50\,\text{g}\,\text{cm}^{-3}$, nitric acid/sample = 100 ml/100—200 mg). In order to assure uniform attack by the acid, the samples were stirred during treatment. After a certain time, the samples were taken out and washed in distilled water for 12 h. Then they were rinsed with acetone in a Soxhlet extractor for 6 h and dried under vacuum at 303 K for 12 h.

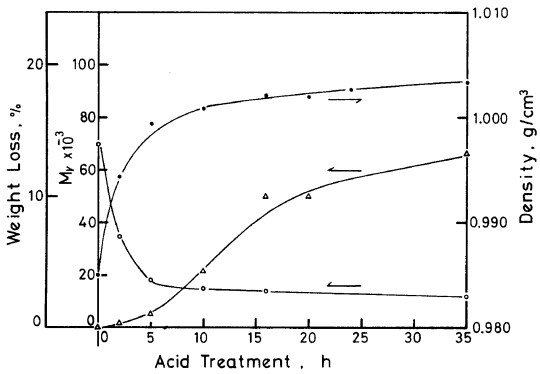

Figure 1. Per cent weight loss (△), viscosity-average molecular weight (○), and density (●) of a pressure-crystallized polyethylene *versus* degradation time in fuming nitric acid.

It is important to note how the oxidation proceeds with time under the conditions used in this study. The sample crystallized at 499 K and 513 MPa for 20 h was tested. The results are shown in Figure 1. The weight loss changed in a sigmoidal fashion with time. After about 10 h, the inflection point appeared at a weight loss of about 4—5%. The density of the original sample was $0.985\,\text{g}\,\text{cm}^{-3}$. In the initial stage, the density increased steeply as a result of removing the amorphous layers between the crystallites and adding polar endgroups of carboxyl and nitro groups on to the cut chain ends. The density appeared to level off at about 1.002 $\text{g}\,\text{cm}^{-3}$ after about 10 h and then increased slightly with time. On the other hand, within several hours M_v decreased very rapidly from the original value of 69,500 to about 18,600, and then changed very slowly. This behavior can be explained by the random scission model,[12] and Keller *et al.*[13] showed the agreement of this behavior with the hypothesis of Ward,[12] *i.e.*, chain scission occurs randomly on carbon–carbon bonds located in a region of the polymer accessible to nitric acid. In this paper, we do not consider any further the kinetics of oxidation of polyethylene by fuming nitric acid.

Gel-Permeation Chromatography

A Waters model 200 gel-permeation chromatograph with a series arrangement of columns of upper porosity rating of 2×10^6, 1×10^5, 6.5×10^4, 9×10^3, and 1×10^3 A was used to measure the GPC of the degraded samples. *o*-Dichlorobenzene was

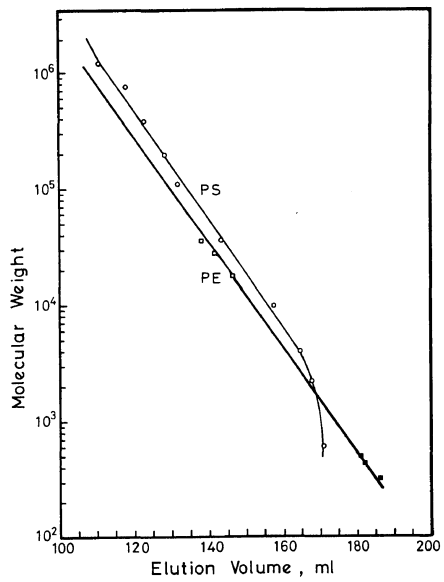

Figure 2. Calibration curves for polystyrene (PS) and polyethylene (PE) at 408 K in *o*-dichlorobenzene: (○) experimental points for PS, (□) experimental points for PE, and (■) experimental points for paraffines. Solid curve for PE was obtained by universal calibration.

used as solvent and the column temperature was set at 408 K. Elutions were conducted at a flow rate of 1 ml min^{-1}. A polymer concentration of about 0.20% (w/v) was employed, and the sample solution in the loop (2 ml) was injected for a period of 2 min. The calibration curve of elution volume *vs.* MW was obtained for standard polystyrenes with narrow MWD, which were purchased from Pressure Chemical Company. Figure 2 shows the calibration curves obtained. These curves are essentially linear in the MW between 3×10^3 and 1×10^6. A linear equation was obtained by the least-square regression,

$$\log M_{PS} = -0.235\times V + 11.348 \qquad (2)$$

where M_{PS} is the MW of standard polystyrene, and V is the elution volume at the peak of a GPC curve.

Grubisic *et al.*[14] reported that the hydrodynamic volume can be used for the universal calibration of GPC, and showed that a plot of log $[\eta]M$ *vs.* V was the same for various homopolymers. At a given elution volume, all polymers are assumed to have the same value of $[\eta]M$, so that we may write,

$$\log [\eta]_{PS}M_{PS} = \log [\eta]_P M_P \qquad (3)$$

where PS refers to the calibration established experimentally with polystyrene standards and P referes to the polymer requiring analysis. It is also assumed that the column combination, solvent, and temperature remain constant. Therefore, eq 3 permits the determination of M_P from an experimental polystyrene calibration, if the dependence of $[\eta]_{PS}$ and $[\eta]_P$ on elution volume can be established. Intrinsic viscosity and MW are related by the familiar equation,

$$[\eta] = KM^{\alpha} \qquad (4)$$

where K and α are the Mark–Houwink constants. Substitution of eq 4 for the two polymers into eq 3 and rearrangement give,

$$\log M_P = \frac{1+\alpha_{PS}}{1+\alpha_P}\log M_{PS} + \frac{1}{1+\alpha_P}\log\frac{K_{PS}}{K_P} \qquad (5)$$

where K_{PS}, α_{PS}, and K_P, α_P are the Mark–Houwink constants for polystyrene and another polymer, respectively. Here, we are concerned with the relations of $[\eta]$ to MW for polystyrene and polyethylene in *o*-dichlorobenzene at 408 K. We used the following two equations for these polymers.[15,16]

$$\text{PS:} \quad [\eta]^{ODCB}_{408\,K} = 1.5084\times10^{-4}M_0^{0.693} \qquad (6)$$

$$M_0 = \sqrt{M_n M_w}$$

where M_0 is an apparent volume peak MW calculated for narrow MW samples for which instrumental M_n and M_w values were determined.

$$\text{PE:} \quad [\eta]^{ODCB}_{408\,K} = 2.0922\times10^{-4}\,M_w^{0.735} \qquad (7)$$

Thus, eq 8 is obtained as,

$$\log M_w(\text{PE}) = 0.975_7\times\log M_0(\text{PS}) - 0.081_9 \qquad (8)$$

Substitution of eq 2 to eq 8 gives,

$$\log M_w(\text{PE}) = -0.229_5\times V + 10.99_0 \qquad (9)$$

Equation 9 was checked by the GPC measurements of several fractionated polyethylenes and paraffins, and was found to be approximately valid as shown in Figure 2. These calibration curves obtained for polystyrene and polyethylene were examined by measuring the NBS standard samples of polystyrene (SRM 705) and polyethylene (SRM 1475). The values of M_w of SRM 705 are estimated to be 179,300 by light scattering and 189,800 by the sedimentation equilibrium method, and the value of

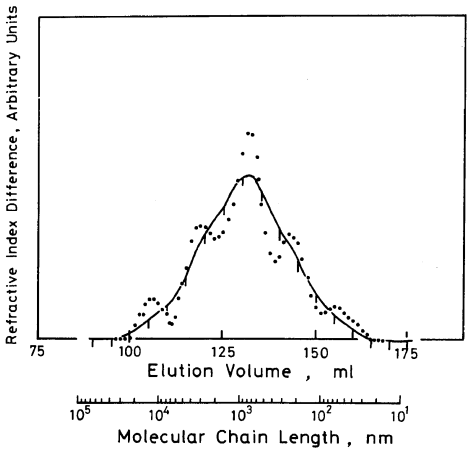

Figure 3. GPC curve of original polyethylene used in this study. Solid circles represent the GPC curve corrected for instrumental spreading.

M_w of SRM 1475 is estimated to be 52,000 by light scattering. The M_w value of this polystyrene was estimated to be 183,500 from our calibration curve of GPC. Hence, the calibration curve for polystyrene was accurate within several percent. On the other hand, the GPC M_w value of the polyethylene was found to be 59,000 and thus about 13% higher than the standard value. This error may be ascribed to the calibration curve determined by inadequate Mark–Houwink constants. In any event, estimation of average MW of polyethylenes in this study was not more accurate than about 13%.

Figure 3 shows the GPC curve of the original sample of polyethylene. An observed GPC curve does not represent a true MWD curve unless the resolution is perfect and ideal. Therefore, correction of observed GPC curve for instrumental spreading is necessary to find the true MWD. The distribution of molecular weight $\omega(y)$ may be considered a continuous function, and it is related to the observed chromatogram $f(x)$ by,

$$f(x)=\int_{\alpha}^{\beta} g(x, y)\omega(y)\,dy \tag{10}$$

where $g(x, y)$ is an instrumental spreading function, and x and y are elution volumes, and α and β are the initial and final volumes of the GPC curve.

Tung *et al.*[17] demonstrated that Gaussian spreading is a good approximation for polyethylene up to a MW of 460,000. We therefore assume for the polyethylene sample,

$$g(x, y)=\sqrt{h/\pi}\exp[-h(x-y)^2] \tag{11}$$

where h is the resolution factor describing the width of the spreading and relates to the standard deviation σ of the Gaussian distribution by,

$$h=1/2\sigma^2 \tag{12}$$

We estimated the resolution factor by fitting the Gaussian distribution to the leading halves of the chromatograms for the standard polystyrene samples.[18] The estimated values of h were approximately equal to 1.3 in the MW range between 6×10^3 and 5.5×10^5. In this study, the constant value $h=1.3$ was assumed for all samples. The correction for instrumental spreading was made by Chang and Huang's method,[19] since this method resolves the oscillation problems encountered in other methods.[20–24] Further, it was shown to be very useful even when resolution was low.

Degradation of polyethylene with fuming nitric acid results in the addition of polar endgroups to the cut polymer chains. It is known that these polar molecules remain in the GPC column longer than the corresponding non-degraded chains, but retention decreases with increasing MW.[25] The peak width and peak elution volume become negligible with increasing MW above about 2,000.[26] In this study, we have neglected the effect of molecular weight spread due to polar endgroups on the GPC curves and also it is assumed that the Gaussian distribution is also applicable to degraded polyethylenes. The precision and efficiency of Chang–Huang's spreading correction for polyethylene were examined by measuring and correcting the GPC curves of a mixture of two fractionated polyethylenes with known MWs. One of the fractionated polyethylenes was a sample of $M_0=27{,}700$, purchased from by Pressure Chemical Co., and another sample of $M_w=126{,}000$ was prepared by column fractionation in our laboratory. The mixture was made by blending the two samples at a ratio of 6 to 4. Figure 4 shows the GPC curves of the two fractionated samples and their mixture. The GPC curve of the mixture was corrected for instrumental spreading by Chang–Huang's method. The corrected GPC curve showed two sharp peaks at positions corresponding to the peaks for the fractionated samples. The M_w values and polydispersity at these peaks were estimated to be $M_w=27{,}700$ and $M_w/M_n=1.22$ for the former

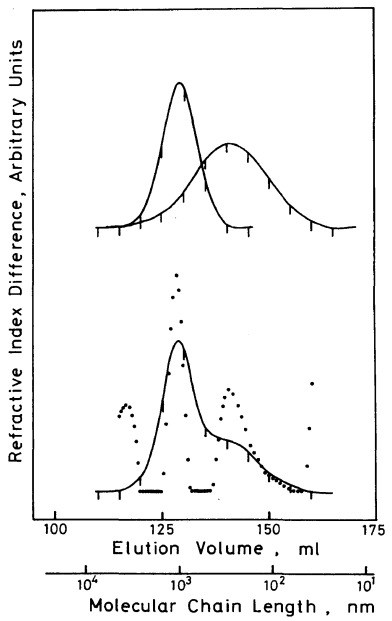

Figure 4. GPC curves of two fractionated polyethylenes and the mixed sample. Solid circles represent the corrected GPC curve.

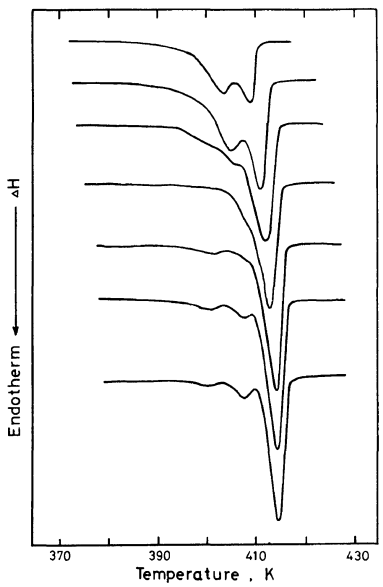

Figure 5. DSC curves for the melting of polyethylene samples formed at 513 MPa under the following conditions (from top to bottom): 433 K for 2 h, 453 K for 20 h, 480 K for 20 h, 491 K for 20 h, 502 K for 20 h, 505 K for 20 h, and 508 K for 20 h. Heating rate, 5 K min^{-1}.

sample and $M_w = 127{,}000$ and $M_w/M_n = 1.02$ for the latter. Figure 4 shows good reproducibility and high resolution attained by the Chang–Huang's correction method. A small peak and an oscillation were detected at the ends of the corrected GPC curve. It is hardly possible that such a peak can exist since it is situated at the point from which the observed GPC curve begins to ascend from or descend to the baseline. Probably, this strange peak and the oscillation are due to a sensitive correction of the GPC curves of low accuracy, especially in the neighborhood of either end of the curves.

RESULTS

Figure 5 shows the DSC curves of the samples crystallized isothermally at various temperatures under a high pressure of 513 MPa. It is well known that the morphological structure and lamellar thickness of the crystals so obtained are strongly dependent upon crystallization temperature. The samples quenched at temperatures below 433 K generally consist of FCC. The DSC curve of the sample quenched at 433 K for 2 h shows two endothermic peaks at about 409 K and 405 K, indicating the fusion of two FCCs. We refer to these as thick FCC and FCC in order to distinguish their respective higher and lower melting points. The samples formed at temperatures above about 453 K contain the so-called ECC in addition to the FCC crystals. The content of the ECC increases with increasing temperature, while that of FCC decreases. For samples formed at temperatures above about 483 K, the DSC curves show a typical pattern with a main peak at about 415 K, and the fracture surfaces of the crystals show typical striated, banded-type lamellar crystallites characteristic of ECC.

Figure 6 shows the GPC curves of the pressure-crystallized polyethylenes degraded with fuming nitric acid at 353 K for 10 h. The GPC curve of the sample formed at 433 K corresponded well to the DSC melting pattern of the original sample. The average chain lengths of the two peaks corresponding to the lamellar thicknesses of thick FCC and FCC were estimated to be 86.5 nm and 29 nm from the corrected GPC curve. This curve also suggests the existence of multiple peaks in the higher MW region. The chain lengths of these peaks were estimated to be 4 times, 5 times, and 8 times the

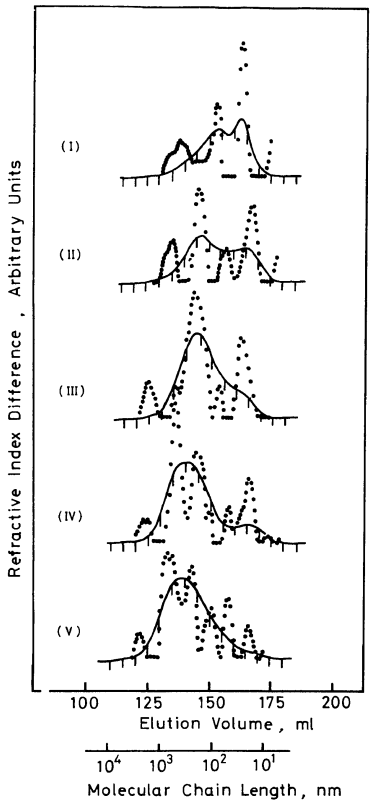

Figure 6. GPC curves of pressure-crystallized polyethylenes degraded with fuming nitric acid at 353 K for 10 h. Figures show chromatograms of samples formed isothermally at 433 K (I), 453 K (II), 480 K (III), 491 K (IV), and 502 K (V) in the order of top to bottom, respectively. Solid circles represent the corrected GPC curves.

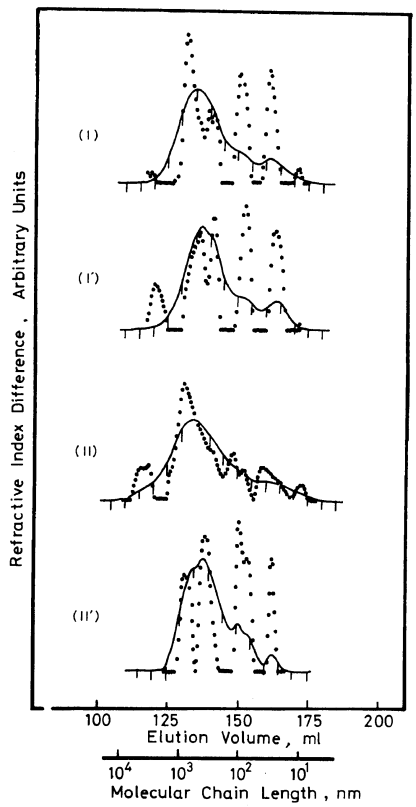

Figure 7. GPC curves of the pressure-crystallized polyethylenes formed at 505 K (I) and 508 K (II) and then treated with fuming nitric acid. Curves (I) and (II) are the GPC curves of the first degraded samples, and the curves (I′) and (II′) are the GPC curves of repeatedly degraded samples.

chain traverse length of thick FCC. The occurrence of these multiple peaks are characteristics of folded-chain structure and these peaks indicate an intermediate stage of fold-cutting in the FCC sample. The sample formed at 453 K for 20 h consisted of FCC and ordinary ECC with melting points of 405 K and 410.8 K. The observed GPC curve of the degraded sample clearly showed two peaks and the distribution pattern corresponded well to the DSC melting pattern of the original sample. The average chain lengths of the two peaks corresponding to the crystal thickness distributions of ordinary ECC and FCC were estimated to be 191 nm and 19 nm from the corrected GPC curve. The corrected curve also suggests the existence of multiple peaks corresponding to triple and quadruple the chain traverse lengths of ordinary ECC and FCC. The DSC melting curve of the sample formed at 480 K for 20 h shows a fusion of FCC and ordinary ECC with melting points of about 403 K and 412 K, respectively. The observed GPC curve of the degraded sample shows a main peak and a shoulder at lower MW. The average chain lengths of ordinary ECC and FCC were estimated to be 230 nm and 28.5 nm from the corrected curve. Two other peaks found on the corrected GPC curve corresponded to triple the chain traverse length of FCC and to twice the chain length of ordinary ECC.

A striking fact can be found in regard to the degraded samples crystallized at temperatures above 491 K: The observed GPC curves showed mainly a large and broad peak suggesting the crystal

thickness distribution of the so-called ECC, but the main peak was found to consist of the two constituents having the crystal thickness distributions of the high ECC and the ordinary ECC on the corrected GPC curves. As is shown in Figure 6 (IV) and Figure 6 (V), the observed curves of the samples formed at 491 K and 502 K for 20 h have a main peak with an average chain length of about 360—380 nm. However, this main peak is found to be split into two peaks when corrected for instrumental spreading, and the average chain lengths of these two peaks are 513 nm and 201 nm in Figure 6 (IV), and 678 nm and 236 nm in Figure 6 (V). In order to observe experimentally these two peaks on GPC, the two samples formed at 505 K and 508 K for 20 h were oxidized thoroughly by repeating of the oxidation process. Figure 7 shows the GPC curves of the degraded samples. Generally speaking, the repetition of the degradation shifts the GPC peaks toward lower MW and causes the peak width to bcome narrower. For the sample formed at 505 K for 20 h, the observed GPC curve of the first degraded sample showed a main peak and two shoulders in the lower MW region, and the corresponding average chain lengths were 563 nm, 104 nm, and 36 nm. On the corrected curve of the first degraded sample, the observed main peak was split into two peaks with an average lengths of 774 nm and 350 nm, besides two sharp peaks at the positions where two shoulders had been observed. By repetition of the degradation, the split main peaks became clearer on GPC, and had average chain lengths of 542 nm and 276 nm besides the two peaks with average chain lengths of 88 nm and 28 nm. For the sample formed at 508 K for 20 h, the observed GPC curve of the first degraded sample showed a pattern similar to the GPC curve of the sample formed at 505 K. The average chain lengths of the observed peaks were 635 nm, 94 nm, and 48 nm. On the corrected GPC curve, the main peak was decomposed into a sharp peak and a shoulder giving average chain lengths of 847 nm and 469 nm, respectively. The GPC curve of the repeatedly degraded sample became narrower and sharper and, at the same time, the split main peaks were seen more clearly. The average chain lengths of these peaks on the corrected GPC curve were 787 nm, 370 nm, 104 nm, (shipping the peak with 78 nm), and 30 nm in the order of decreasing MW.

Figure 8 shows the temperature dependence of the average chain lengths of various crystals estimated from the peaks on the corrected GPC curves. The crystal thickness of ordinary ECC increased gradually in the temperature region between 453 K and 493 K and approached about 240 nm. However, the crystal thickness of FCC increased only slightly. At high temperatures above about 493 K, new crystals of ECC and FCC were formed besides ordinary ECC and FCC. The crystal thicknesses of ordinary ECC and new ECC increased steeply with increasing temperature above 503 K.

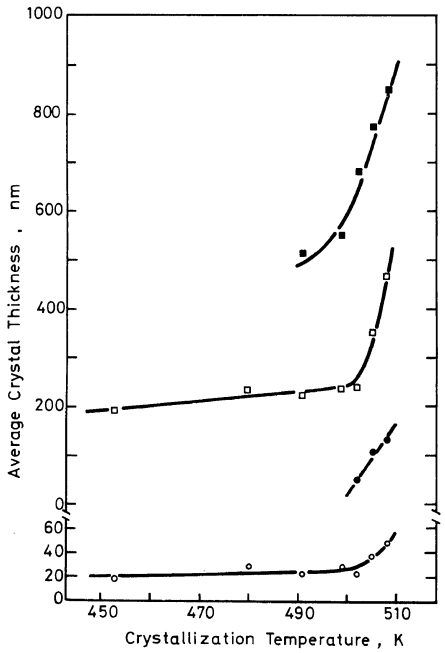

Figure 8. Variation in average crystal thickness of various crystals with crystallization temperatures: (■), high ECC; (□), ordinary ECC; (●), thick FCC; (○), FCC.

Figure 9 shows the degradation time dependence of the GPC curve of the degraded sample which was cooled slowly from the melt at 513 MPa. During a short period of degradation, the GPC curves showed a main peak and two ambiguous shoulders in the lower MW region. With an increase in the degradation time to more than 24 h, the main peak split into two peaks. These split peaks may be associated with the crystal thickness distribution of high ECC and ordinary ECC. Figure 10 shows the average chain lengths of these peaks as a function of

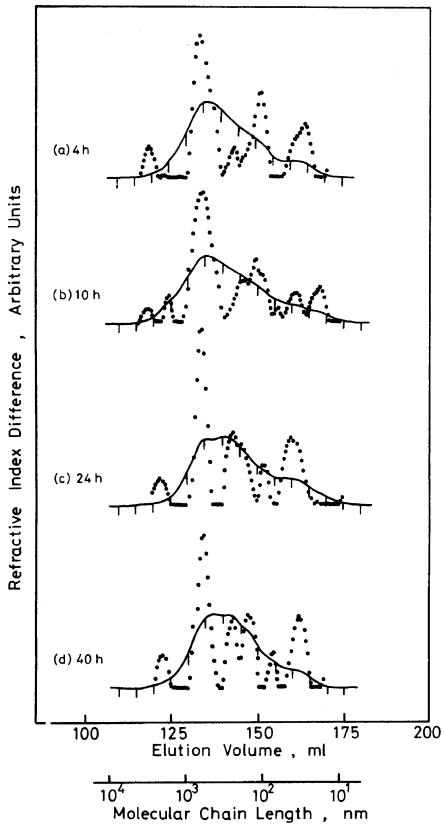

Figure 9. GPC curves of polyethylene cooled from the melt at 513 MPa and then degraded with fuming nitric acid for (a) 4 h, (b) 10 h, (c) 24 h, and (d) 40 h.

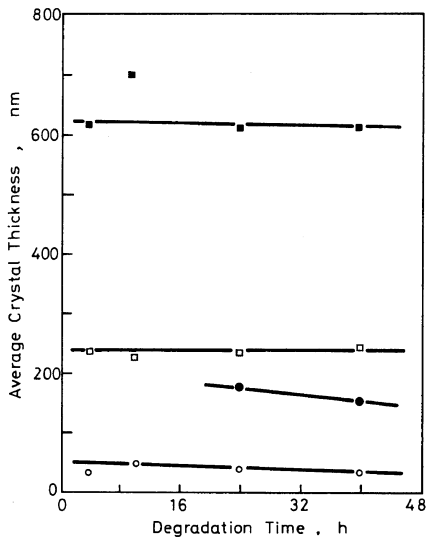

Figure 10. Degradation time dependence of average crystal thickness for the crystals in the sample cooled from the melt at 513 MPa: (■), high ECC; (□), ordinary ECC; (●), thick FCC; (○), FCC.

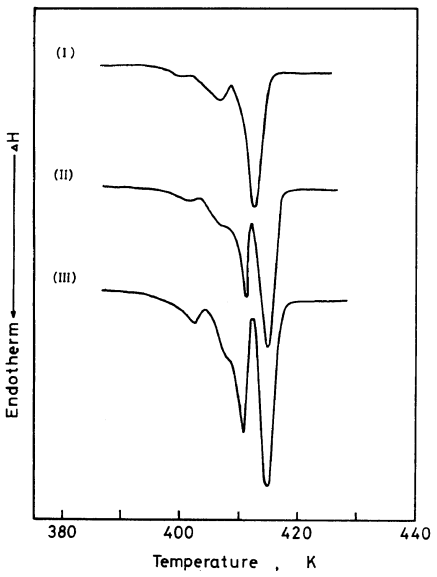

Figure 11. DSC curves for the melting of polyethylenes crystallized at 507 K and 513 MPa for (I) 1 h, (II) 100 h, and (III) 235 h.

degradation time. The average crystal thicknesses of high ECC, ordinary ECC, thick FCC, and FCC in the original sample were estimated to be 620 nm, 240 nm, indeterminate, and 35 nm, respectively, by extrapolation to zero degradation time.

We reported in a previous paper[27] that when polyethylene is crystallized under slight supercoolings for a long time at about 500 MPa, high ECC and ordinary ECC are formed separately by the individual crystallization processes. This was demonstrated by the exceptional melting behavior on the DSC curves at atmospheric pressure and also on the dilatometric curves under high pressures. The DSC curves showed two main peaks at about 413 K and 417 K, indicating the fusion of ordinary ECC and high ECC. In order to determine the average crystal thicknesses of the two ECC crystals in these samples, they were crystallized at 507 K and 513 MPa for periods of 1 h, 100 h, and 235 h. Figure 11 shows the DSC melting curves of these samples. We have already reported that the main peak changes to

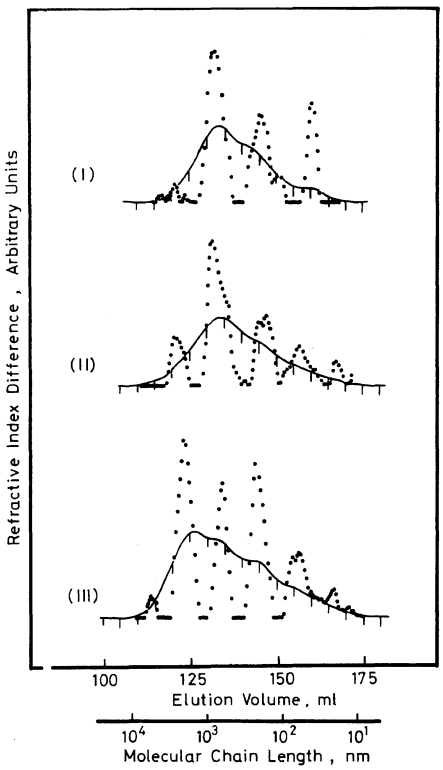

Figure 12. GPC curves of polyethylenes crystallized at 507 K and 513 MPa for (I) 1 h, (II) 100 h, and (III) 235 h and then degraded with fuming nitric acid for 10 h.

two sharp endothermic peaks with increasing crystallization time. Figure 12 shows the GPC curves for these samples degraded at 353 K for 10 h. For the degraded sample formed for 1 h, the GPC curve showed a main MWD peak and two ambiguous shoulders in the lower MW region, and these three peaks corresponded to average chain lengths of 754 nm, 181 nm, and 36 nm on the corrected curve, and to the crystal thickness distributions in ECC, thick FCC, and FCC, respectively. The main peak corresponding to the average chain length of ECC showed a strong peak on the corrected GPC curve. The MWD pattern of the GPC curve corresponded well to the DSC melting pattern of the original sample. For the degraded sample formed for 100 h, the observed GPC curve was similar to that for the sample formed for 1 h, and the average chain lengths of the three peaks were 795 nm, 191 nm, and 54 nm on the corrected curve. At this stage, it should be noted that the main peak on the observed GPC curve had a tail toward higher MW and that this tail was taken as a peak with the average chain length of about 2 μm on the corrected curve. For the degraded sample formed for 235 h, the tail grew to be the strongest peak in the observed and corrected curves, and the whole distribution pattern became more clear. Since the corrected GPC curve corresponded well to the DSC melting pattern of the original sample, the strongest peak can be regarded as the crystal thickness distribution of high ECC and the other three peaks are regarded as the crystal thickness distributions of ordinary ECC, thick FCC, and FCC in the order of decreasing MW. The average chain lengths of these peaks were estimated to be 1.85 μm, 594 nm, 212 nm, and 58 nm. It is very interesting to note that an enlargement in the highest MW peak with increasing crystallization time is consistent with the change in melting pattern of the sample on the DSC curves. The enlargement of this peak strongly suggests crystal growth in high ECC during the isothermal crystallization at 507 K for prolonged periods of time.

Table I gives the data for the average crystal thickness and its size distribution in the molecular chain direction of various crystals in the pressure-crystallized polyethylenes. Peak chain length L_{peak} indicates the mean value of crystal thickness for each crystal. In regard to each MWD peak of each crystal, the half width, the ratio of maximum to minimum chain length L_{max}/L_{min}, and the polydispersity M_w/M_n were estimated to obtain information on the crystal thickness distributions in various crystals.

DISCUSSION

It is well known that pressure-crystallized polyethylenes generally consist of several types of crystals with a different morphological structure and different average crystal thickness. Statistical analysis of the crystal thickness and its size distribution in various crystals in these complex systems has been made by fuming nitric acid degradation followed by GPC measurement of MWD of the degraded samples. By using Chang–Huang's method, we generally succeeded in correcting the observed GPC curves for instrumental spreading. But the correction often brought about strange peaks and oscillations at the ends of the

Table I. Parameters of each MWD peak on corrected GPC curves that correspond to crystal thickness distributions in degraded pressure-crystallized polyethylenes

Crystallization at 513 MPa		Acid treatment at 353 K	Crystal type		L_{peak}	Half width	Range	L_{max}/L_{min}	M_w/W_n
					nm	nm	nm		
Temp/K	Time/h	Time/h							
433	2	10	Thick	FCC	86.5	36	64.5— 132	2.05	1.02_3
				FCC	29	10	21 — 38	1.81	1.01_5
453	20	10	Ordinary	ECC	191	94	122 — 284	2.33	1.03_1
				FCC	19	11	13 — 37	2.85	1.04_4
480	20	10	Ordinary	ECC	230	209	122 — 456	4.07	1.08_9
				FCC	28.5	28	15 — 50	3.33	1.05_6
491	20	10	High	ECC	513	245	291 — 838	2.88	1.04_1
			Ordinary	ECC	201	122	99 — 333	3.36	1.04_4
				FCC	28	13	14 — 34	2.61	1.04_1
502	20	10	High	ECC	678	510	315 —1010	3.21	1.05_1
			Ordinary	ECC	236	126	163 — 400	2.45	1.02_9
				FCC	49.5	19	34 — 68	2.00	1.01_6
505	20	10	High	ECC	774	385	433 —1150	2.66	1.03_5
			Ordinary	ECC	350	136	212 — 481	2.27	——
			Thick	FCC	104	54	70 — 150	2.14	1.02_9
				FCC	36	14	23.5— 48	2.04	1.02_2
508	20	10	High	ECC	847				
			Ordinary	ECC	469				
			Thick	FCC	131		Ambiguous		
				FCC	47				
508	20	2 × 10	High	ECC	787	385	521 —1035	1.99	1.02_4
			Ordinary	ECC	370	174	212 — 507	2.39	1.03_1
			Thick	FCC	104	32	72 — 128	1.78	1.03_7
				FCC	30	7	24 — 36	1.50	1.00_6
Cooled		40	High	ECC	610	238	379 — 957	2.52	1.03_1
			Ordinary	ECC	242	96	186 — 341	1.83	1.01_6
			Thick	FCC	153	69	110 — 224	2.04	1.02_1
				FCC	32	17	22 — 50	2.27	1.05_1
507	1	10	Ordinary	ECC	734	410	422 —1246	2.95	1.04_6
			Thick	FCC	181	116	116 — 299	2.58	1.04_2
				FCC	36	13	29 — 51	1.76	1.01_5
507	235	10	High	ECC	1850	1010	1180 —2900	2.46	1.03_4
			Ordinary	ECC	594	239	433 — 907	2.10	1.02_1
			Thick	FCC	212	98	125 — 315	2.52	1.03_4
				FCC	58	40	37 — 96	2.60	1.03_9

chromatograms. For example, the corrected curves shown in Figure 6 (I) and Figure 6 (II) diverge at the low MW end, while those in Figure 6 (III)—6 (V), Figure 7 (I′), and Figure 9 show spurious peaks at the high MW end. These may have arisen from the low precision of the raw GPC curves.

We could first determine that high ECC and ordinary ECC in a same sample have characteristic crystalline lamellae with different average thicknesses and size distributions, although the for-

mations of the two ECC crystals were already detected by DSC and high-pressure dilatometry. Furthermore, it was surprising that even for samples formed at lower temperatures between 493 K and 505 K at 513 MPa for 20 h, which showed only a fusion of the so-called ECC besides the melting of FCC crystals, two split peaks could be clearly seen on the corrected GPC curves and often on the observed GPC curves. In these cases, it is reasonable to assign the two split peaks to the crystal thickness distributions of high ECC and ordinary ECC. The fact that two peaks corresponding to the chain lengths of high ECC and ordinary ECC appear at wider temperatures under 513 MPa was unexpected as has already been stated in the previous paper.[27] This situation would not become evident by conventional fracture surface observation. In the samples formed at temperatures between 493 and 508 K, the crystal thickness of high ECC increased from *ca.* 500 to *ca.* 800 nm, while the thickness of ordinary ECC increased from *ca.* 230 to 470 nm. The lamellar thickness of thick FCC also increased from *ca.* 85 to *ca.* 280 nm and also FCC was thickened from *ca.* 19 to *ca.* 47 nm in the same temperature region.

In complex systems such as the pressure-crystallized polyethylenes, the crystal thickness of a certain crystal may overlap that of other crystals formed under different conditions. Figure 13 compares the peaks of four kinds of crystals in the various samples. The thick FCC and the ordinary ECC formed at 507 K for a long period of time have average crystal thicknesses comparable to those of ordinary ECC and high ECC in other samples. As can be seen in Figure 13, the classification into four categories of high ECC, ordinary ECC, thick FCC, and FCC has only relative meaning. According to the definition by Wunderlich,[28] the term ECC is applid to any crystal with sufficiently high MW having a crystal thickness of at least 200 nm. In this sense, thick FCC may often be regarded as ECC. After all, the experimental results in this study reveal that the real crystals in the pressure-crystalized samples will have various chain extensions in the crystalline lamellae in the molecular chain direction. It is interesting to note that these crystals have distinct average lamellar thicknesses and size distributions.

Concerning the ratio of average crystal thicknesses of different crystals in a sample, it was found that the average crystal thickness of ordinary ECC

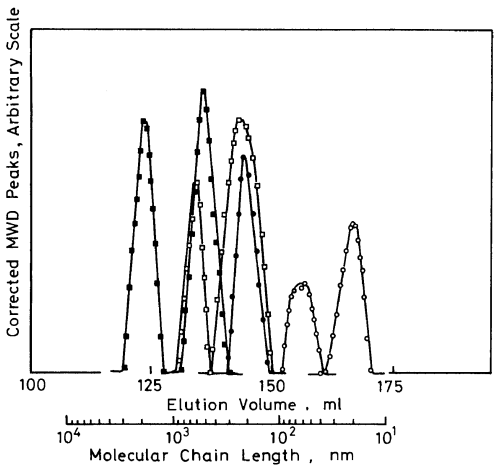

Figure 13. Representative curves of the corrected MWD peaks of the four kinds of crystals: high ECC (■), ordinary ECC (□), thick FCC (●), and FCC (○).

is between one half and one third the average thickness of high ECC. A more precise analysis showed that the average thickness of ordinary ECC was nearly equal to one half the average thickness of high ECC in the samples formed at relatively high temperatures. However, this ratio in the sample formed at 507 K for a prolonged time was one third. This change implies a remarkable crystal thickening of high ECC during prolonged isothermal crystallization. In the sample cooled from the melt, the ratio was intermediate between one half and one third. Similar simple relations seem to hold for other crystals. The ratio of average crystal thicknesses between FCC and thick FCC was nearly one third. On the other hand, the ratio of crystal thicknesses between FCC and ordinary ECC scattered, but the ratio of one tenth was often found. These results imply that when polyethylene is crystallized from the melt under high pressures, the lamellar thicknesses of the crystals formed in the later crystallization processes are influenced strongly by the high ECC formed initially. At least, it can be assumed that ordinary ECC has a lamellar thickness from one half to one third the crystal thickness of high ECC.

Figure 14 shows the half part of crystal thickness distribution for various crystals of different samples. Ward and Williams[29] discussed the possible causes of molecular weight spread of GPC peaks of the degraded FCC samples: first, variation in the crystal

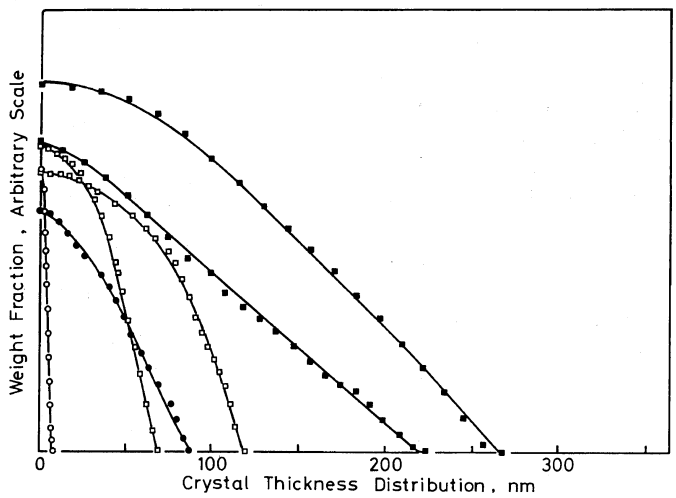

Figure 14. Representative distributions of half MWD peaks of the four kinds of the crystals arranged in the same peak position.

thickness of the original crystal and second, variation in the depth beneath the lamellar surfaces of chain ends or variation in a long accessible loop. In the cases of ECC which may contain a small number of folds, fluctuation due to the second cause would be negligible in relatively degraded stages. Strictly speaking, the appropriate condition for the degradation of a crystal in which amorphous layers and folds can be cut and also in which the crystal core is protected, may be different for each sample. In the case of FCC, the nitric acid degradation at 353 K for 10 h was insulfficient since the GPC curves as illustrated in Figure 6 (I) and Figure 6 (II) indicate the existence of uncut folds. The degradation condition in this study was, however, generally appropriate for the ECC samples in the pressure-crystallized polyethylenes, except for those cases shown in Figure 7 (II) and Figure 9 (b). The molecular weight spread may thus be ascribed to fluctuation in the crystal thickness of ECC. As shown in Figure 14, the absolute crystal thickness distribution broadened greatly with increasing average crystal thickness. The values of L_{max}/L_{min} varied from 2.0 to 4.0 among the crystals. The ratio for high ECC ranged from 2.0 to 3.2, but the polydispersity M_w/M_n was surprisingly small and was lower than 1.05. On the other hand, the L_{max}/L_{min} value for ordinary ECC decreased from 4.1 to 2.3 with increasing crystallization temperature. The reason for this is that a considerable MW spectrum in polyethylene is contained in ordinary ECC at the lower crystallization temperatures, while at the higher temperatures, fractional crystallization into four kinds of crystals proceeds remarkably. The value of L_{max}/L_{min} and M_w/M_n of FCC were distributed over 1.8—3.3, and 1.01—1.06, respectively. These data indicate clearly that the crystal thickness distributions of all the crystals, especially that of ordinary ECC and high ECC, are statistically narrow, comparable to the MWD of anionically polymerized polystyrenes.

The surface structure of ECC has been explored with a great interest in the past, but little information has so far been obtained in that no adequate method has been available. Since the crystal thickness of ECC, especially that of high ECC, is generally comparable to or greater than the average molecular chain length of original material, straight stems of crystalline lamellae may be largely terminated in the form of extended chains. Under these circumstances, chain ends of straight stems can be easily distributed in the neighborhood of the crystal surfaces, and the disordered surface layers will be relatively thicker than the surface layers in FCC. In fact, the surface layer of high ECC was estimated to be from 10 to 20 nm in the sample cooled from the melt at 513 MPa. It seems reasonable that high ECC may have a surface layer of about 20 ± 10 nanometers including a completely disordered amorphous layer. It is very interesting to note that the

existence of such long disordered surface layers on high ECC and also on ordinary ECC may be related closely to the easy occurrence of hexagonal modification of polyethylene under high pressure and high temperature.[30,31]

Acknowledgement. The authors wish to thank Professor R. Y. M. Huang of the University of Waterloo for kindly permitting us to use the computer programs for calculating true molecular weight distributions from observed GPC curves. The authors also wish to thank Dr. S. Hattori of National Chemical Laboratory for Industry for providing several standard polystyrene samples.

REFERENCES

1. R. B. Prime and B. Wunderlich, *J. Polym. Sci., A-2*, **7**, 2061 (1969).
2. D. V. Rees and D. C. Bassett, *J. Polym. Sci., A-2*, **9**, 385 (1971).
3. T. Williams, D. J. Blundell, A. Keller, and I. M. Ward, *J. Polym. Sci., A-2*, **6**, 1613 (1968).
4. T. Williams, A. Keller, and I. M. Ward, *J. Polym. Sci., A-2*, **6**, 1621 (1968).
5. F. M. Willmouth, A. Keller, I. M. Ward, and T. Williams, *J. Polym. Sci., A-2*, **6**, 1627 (1968).
6. D. M. Sadler, T. Williams, A. Keller, and I. M. Ward, *J. Polym. Sci. A-2*, **7**, 1819 (1969).
7. K. H. Illers, *Makromol. Chem.*, **118**, 88 (1968).
8. D. C. Bassett, B. A. Khalifa, and R. H. Olley, *Polymer*, **17**, 284 (1976).
9. Y. Maeda and H. Kanetsuna, *J. Polym. Sci., Polym. Phys. Ed.*, **12**, 2551 (1974).
10. R. Chiang, *J. Phys. Chem.*, **69**, 1645 (1965).
11. R. P. Palmer and A. J. Cobbold, *Makromol. Chem.*, **74**, 174 (1964).
12. I. M. Ward and T. Williams, *J. Polym. Sci., A-2*, **7**, 1585 (1969).
13. A. Keller and Y. Udagawa, *J. Polym. Sci., A-2*, **9**, 1793 (1971).
14. Z. Grubisic, P. Rempp, and H. Benoit, *J. Polym. Sci., B*, **5**, 753 (1967).
15. D. J. Pollock and R. F. Kratz, paper presented at the 6th International Seminar on GPC, Miami Beach, October 1968.
16. J. C. Moore, *J. Polym. Sci., A*, **2**, 835 (1964).
17. L. H. Tung, J. C. Moore, and G. W. Knight, *J. Appl. Polym. Sci.*, **10**, 1261 (1966).
18. L. H. Tung and J. R. Runyon, *J. Appl. Polym. Sci.*, **13**, 2397 (1969).
19. K. S. Chang and R. Y. M. Huang, *J. Appl. Polym. Sci.*, **13**, 1459 (1969).
20. M. Hess and R. F. Kratz, *J. Polym. Sci., A-2*, **4**, 731 (1966).
21. W. N. Smith, *J. Appl. Polym. Sci.*, **11**, 639 (1967).
22. H. E. Pickett, M. J. R. Cantow, and J. F. Johnson, "Analytical Gel Permeation Chromatography," J. F. Johnson and R. S. Porter, Ed., John Wiley & Sons, Inc., New York, N.Y., 1968, No. 21, 67.
23. P. E. Pierce and J. E. Armonas, "Analytical Gel Permeation Chromatography," J. F. Johnson and R. S. Porter, Ed., John Wiley & Sons, Inc., New York, N.Y., 1968, No. 21, 23.
24. J. H. Duerksen and A. E. Hamielec, "Analytical Gel Permeation Chromatography," J. F. Johnson and R. S. Porter Ed., John Wiley & Sons, Inc., New York, N.Y., 1968, No. 21, 83.
25. F. C. Frank, I. M. Ward, and T. Williams, *J. Polym. Sci., A-2*, **6**, 1357 (1968).
26. T. Williams, Y. Udagawa, A. Keller, and I. M. Ward, *J. Polym. Sci., A-2*, **8**, 35 (1970).
27. Y. Maeda and H. Kanetsuna, *J. Polym. Sci., Polym. Phys. Ed.*, **14**, 2057 (1976).
28. B. Wunderlich and T. Davidson, *J. Polym. Sci., A-2*, **7**, 2043 (1969).
29. I. M. Ward and T. Williams, *J. Macromol. Sci., Phys.*, **B5**, 693 (1971).
30. K. Takamizawa, Y. Urabe, and H. Hasegawa, *Polym. Prepr., Jpn.*, **28**, (9) 1854 (1979).
31. Y. Maeda, H. Kanetsuna, K. Nagata, K. Matsushige, and T. Takemura, to be published.